Journal of Materials Science: Materials in Electronics (2020) 31:9969–9973
https://doi.org/10.1007/s10854-020-03590-6

REVIEW

Swanepoel method for AlInN/AlN HEMTs

Omer Akpinar[1,2] · Ahmet Kürsat Bilgili[1] · Umran Ceren Baskose[2] · Mustafa Kemal Ozturk[1,2] · Suleyman Ozcelik[1,2] · Ekmel Ozbay[3]

Received: 12 March 2020 / Accepted: 12 May 2020 / Published online: 19 May 2020

Abstract
In this study, AlInN/AlN high electron mobility transistor (HEMT) structure is grown on c-oriented sapphire substrate using metal organic chemical vapor deposition method. Optical properties of the structure are investigated by photoluminescence (PL) and ultraviolet (UV–Vis.) spectras. According to PL results, direct bandgap of AlN is determined around 2.80 eV. In UV–Vis. spectra it is seen that conduction of AlInN layer starts at 360 nm. Swanepoel envelope method is applied on transmission spectra and some optical properties such as refractive index (n), film thickness (t), absorption coefficient (α), and extinction coefficient (k) are determined. Forbidden energy bandgap is determined again from Tau method and it is compared with the value gained from PL spectra. This study is a rare one that presents optical properties of HEMTs using Swanepoel and Tau methods. In addition to this, it helps estimating how optical properties of HEMTs effect electrical properties.

1 Introduction

In semiconductor technology, silicon-based materials play a crucial role. All integrated circuits and micro-chips are developed as silicon-based structures. In the last 20 years, III–V group semiconductors also gained importance. As (arsenide)-based AlGaInAs and P (phospate)-based AlGaInP systems are used in high frequency devices, red, and yellow region optoelectronic applications efficiently [1]. However, there are many fields that conventional III–V group semiconductors are not used. Color screens, laser printers, high density data storage, and under-water communication are fields those need short wavelength light emitters. Automobile motors, power distribution systems, and all electrical devices need high power and high temperature transistors. Si and conventional III–V group semiconductors are not convenient for designing optoelectronic devices that operates in blue and ultraviolet region. Gallium arsenide (GaAs)-based electronic devices cannot operate at high temperature. Group III nitrites are convenient in this field. Group III nitrites have large and direct bandgap [2]. Bandgap values of wurtsite semiconductors are 0.7 eV for InN, 3.4 eV for GaN, 6.2 eV for AlN [3]. Because of wide bandgap and strong bond properties, Group III nitrites can be used for blue and green light emitting devices, high temperature transistors. Group III nitrites such as GaN, InN, and AlN also have properties such as wide bandgap and important polarization effects stemming from their hexagonal structure [4].

Towards the end of twentieth century, Shuji Nakamura made it easier to grow GaN epitaxial layer on sapphire substrate using MOCVD method [5]. GaN-based structures presented innovations for improving new optoelectronic devices. At the same time, it is noticed that GaN has perfect electronic properties with its high electron mobility and carrier density for continuous electric fields [6]. To combine, the properties mentioned above is possible with GaN-based HEMTs. Their power density may be increased.

This study is important for relating optical properties with electronic properties of HEMTs. Because of simple and certain measurement property of PL, it is most common characterization technique for optical measurements. By using PL, it is possible to determine bandgap, defect and dirt situations for bulk and layers of semiconductor thin films [7]. Semiconductor materials having direct bandgap, can be excited with high energy photons. In this situation, some of the electrons in valance band are transmitted to conduction band and holes are formed in valance band. That is electron–hole pairs (EHPs) are formed in the semiconductor. For absorption, photon energy should be larger than bandgap

✉ Omer Akpinar
omerakpinar9@gmail.com

[1] Physics Department, Gazi University, Ankara, Turkey

[2] Photonics Research Center, Gazi University, Ankara, Turkey

[3] Physics Department, Bilkent University, Ankara, Turkey

($hf > E_g$). Here h is Planck constant and f is the frequency of photon.

Properties such as bandgap and refractive index can be determined from absorption and transmission spectras. For transmission measurements, light source can produce light in 190–1200 nm wavelength range [8].

For determining refractive index(n), absorption coefficient(α), extinction coefficient(k), and film thickness(t), a simple method called Swanepoel envelope method (or turning point) is used by Lyasenko and Miloslavskii [9] as the first time. Later, this method is improved by Manifacier [10]. This method takes into account only maximum and minimum points in transmission fringes. It is useful for gaining absorbtion coefficient, film thickness, and refractive index with high accuracy. This method is valid only in low extinction coefficient region. It is convenient for films those have less refractive index from the substrate. Equations for this method are applied by Swanepoel as first time in the literature [11].

2 Experimental

AlN and AlInN layers are grown on (00.1) oriented sapphire wafer using MOCVD method. TMGa, TMIn, TMAl, and NH_3, Al, N sources are used and H_2 is used as carrier gas. Before growth of epitaxial film, to remove dirts, sapphire wafer is annealed for 10 min at 1100 °C. AlInN HEMT structures are labeled as sample A and B. Schematic diagrams of sample A and B are shown in Fig. 1. Sample A is formed with sapphire substrate, AlN nucleation layer, and AlN buffer layers. For this sample, first thin Al nucleation layer is grown at low temperature. Later, thick AlN buffer layer is grown at high temperature.

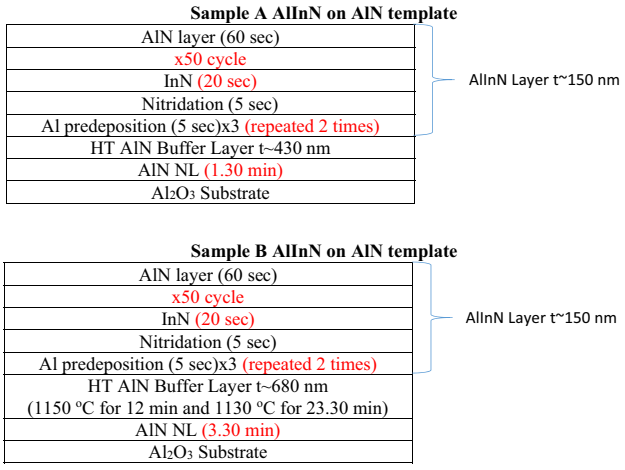

Fig. 1 Schematic diagrams of samples A and B

Sample B is also grown under similar conditions. But sample B does not contain predeposition and nitridation.

3 Results and discussion

Investigation of optical properties is not only for finding basic physical properties but also to determine interesting technological properties. Optoelectronic technology has a dense interest in materials with weak absorbtion in visible and infrared region. Optical constants such as refractive index (n) and extinction coefficient (k) can be determined with different methods. Extinction coefficient (k) can be determined by the help of absorbtion coefficient (α) with relation $4\pi\lambda/\alpha$. Film thickness can also be determined with these methods [12].

Optical transmission spectra can be separated in two regions as weak and strong absorbtion fields. In weak absorbtion region ($\alpha t << 1$), n of the film, α and t can be determined using maximum and minimum points of interference fringes in transmission spectra. This is called as Swanepoel envelope method. Maximum T_M and minimum T_m interference fringe functions are given in Eqs. (1) and (2) [13].

$$T_M = \frac{Ax}{B - Cx + Dx^2} \tag{1}$$

$$T_m = \frac{Ax}{B + Cx + Dx^2} \tag{2}$$

Point values of T_M and T_m can be determined from transmission plot (Fig. 2) without using A, B, C, and D constants in these equations. In middle and weak absorbtion regions, α is not zero and $x << 1$.

By using Fig. 2, n can be determined by the help of a nameless parameter N with Eqs. (3) and (4) [11, 12].

$$N = 2n_s \frac{T_M - T_m}{T_M x T_m} + \frac{n_s^2 + 1}{2} \tag{3}$$

In Eq. (3), n_s is the refractive index of substrate (sapphire).

$$n = [N + (N^2 - n_s^2)^{1/2}]^{1/2} \tag{4}$$

t can be determined from n and λ values of two adjacent fringes. n and λ values can be determined from n versus λ plot. Measurements can be made several times and average value of these measurements gives more accurate value of film thickness. Film thickness can be determined with Eq. (5) [14].

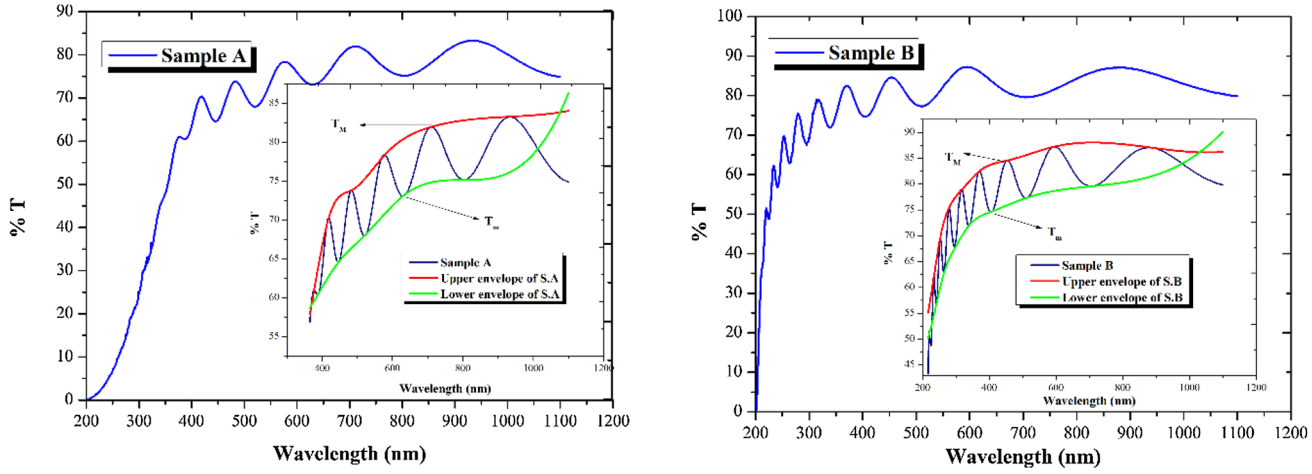

Fig. 2 Transmission spectras of sample A and B

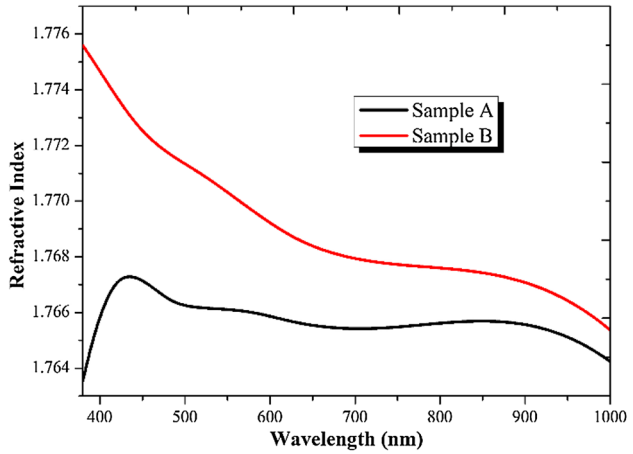

Fig. 3 Refractive index versus wavelength for sample A and B

$$t = \frac{\lambda_1 x \lambda_2}{2(\lambda_1(n_2) - \lambda_2(n_1))} \tag{5}$$

In Fig. 3, n values versus wavelength is shown. Differences in n values may be caused from difference in contents. Fluctuations in n values of sample B may be caused from the inhomogeneity of In content in layers. As can be seen in Fig. 3, there is a peak around 450 nm wavelength for sample A. The reason for occurring of this peak may be dislocations or density of impurities. The description of refractive index is the ratio between speed of light at vacuum and in material. So when the wavelength of the incident beam reaches around 450 nm it propagates slower in the material of sample A. For sample B, the same situation is not present. Refractive index versus wavelength changes more uniformly than sample A. This shows that transparency and in content homogeneity is better in sample B.

Table 1 T values for S.A and S.B

Wavelength (nm)	T_M (S.A)	T_m (S.A)	T_M (S.B)	T_m (S.B)
413	69.3429	62.3497	88.0419	79.5341
412	69.1612	62.2760	88.0408	79.5276
411	68.9753	62.2020	88.0396	79.5211
410	68.7852	62.1278	88.0383	79.5146
409	68.5912	62.0533	88.0369	79.5081
408	68.3934	61.9786	88.0354	79.501
407	68.1918	61.9037	88.0337	79.4950
406	67.9865	61.8285	88.0320	79.4885
405	67.7778	61.7532	88.0302	79.4820
404	67.5658	61.6777	88.0282	79.4754
403	67.3504	61.6020	88.0261	79.4688
402	67.1320	61.5261	88.0240	79.4622
401	66.9105	61.4501	88.0217	79.4556

Absorbtion coefficients are determined using Eq. (6) and (7) with a nameless parameter of E_M [15].

$$E_M = \frac{8n^2 n_s}{T_M} + (n^2 - 1)(n^2 - n_s^2) \tag{6}$$

$$X(\lambda) = \exp(-\alpha t) = \frac{E_M - [E_M^2 - (n^2 - 1)^3 (n^2 - n_s^4)]^{1/2}}{(n-1)^3 (n - n_s^2)} \tag{7}$$

Maximum and minimum fringe points gained from transmission spectra, refractive indexes, absorbtion coefficients, and extinction coefficients are given in Table 1. Average value of t is found as 167 µm.

In weak absorbtion region, wavelength versus α can be determined by $k = 4\pi\lambda/\alpha$. From the plot dependent on α in

Fig. 4, forbidden energy bandgap can be calculated. In this plot, *x*-axis interception point of high energy region fit gives bandgap value.

Bandgap values can also be determined from photoluminescence (PL) spectra. Because of strong and simple measurement properties, for III-group nitrite semiconductors and alloys, it is the most common characterization technique. PL uses light with a convenient energy for measurement [16]. Excited electrons in valance band loses their energy as phonons in semiconductor and conduction band energy goes through minimum electron energy situation. PL measures the system as a function of wavelength. Wavelength in PL spectra can be converted to energy scale using $\lambda = hxc/E$ equation. Energy gained from PL peaks, can be used for determining bandgap values, impurity, and defect levels in interfaces. At the same time, quality of the material can be estimated from density of PL peak and full width at half maximum (FWHM). Narrow and sharp peaks are indicators of good quality in materials. Maximum peak center gives forbidden energy bandgap. This situation is shown in Fig. 5.

4 Conclusion

AlInN/AlN structures are grown using MOCVD technique. n, α are determined by using Swanepoel method applied on transmission spectra. In near infrared and visible region, sharp bended interference fringes are seen in transmission spectra at room temperature. Refractive index values are found around 1.768, mean value of film thickness is found as 167 µm. α and k values of the structures are shown in Table 1. It is seen that bandgap values gained from Tau method and PL spectra are in good accordance. This study

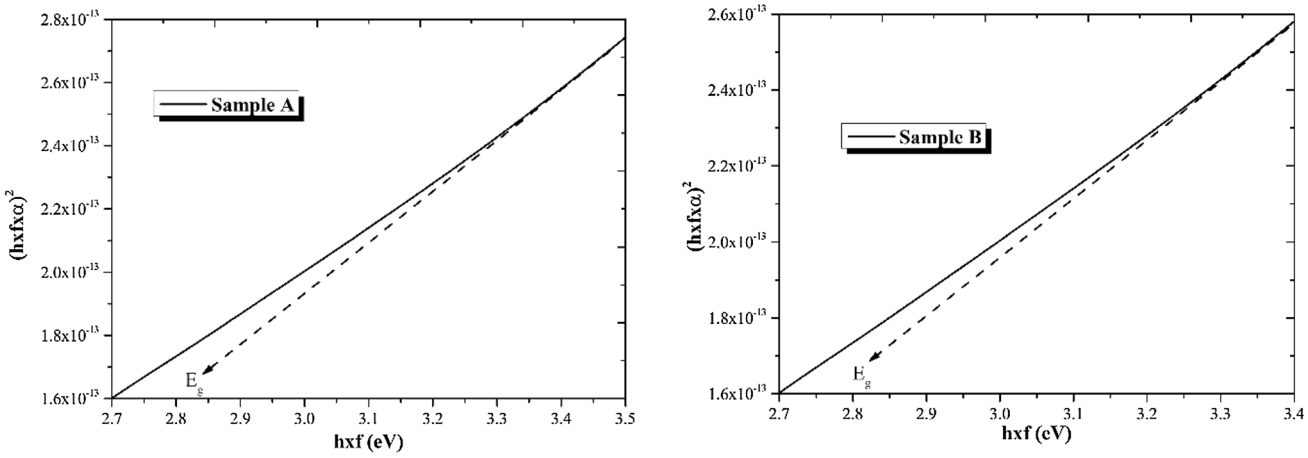

Fig. 4 Tau plots for sample A and B

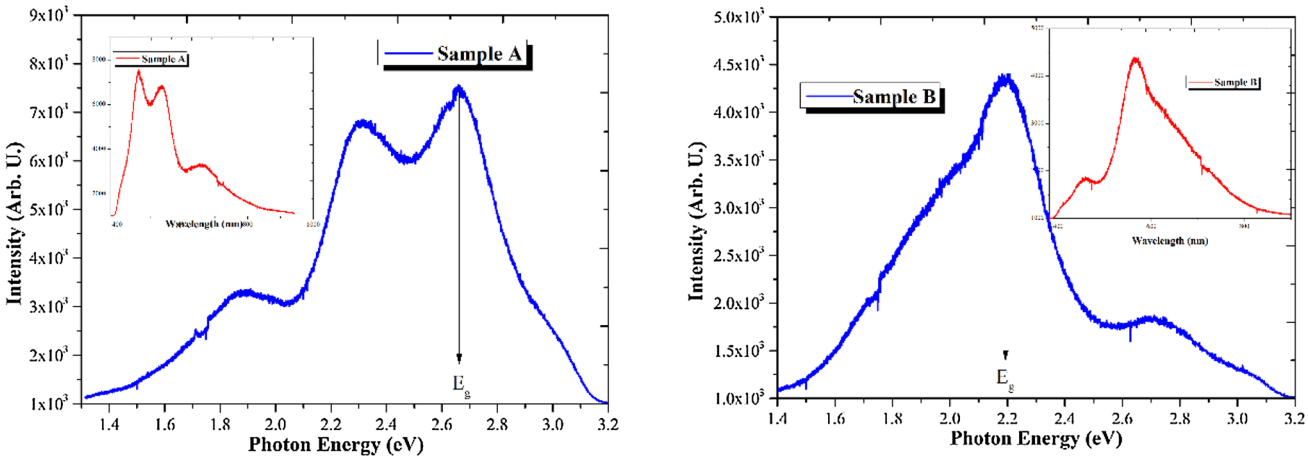

Fig. 5 PL spectras of sample A and B

plays a key role for researchers trying to relate optical and electrical properties of HEMTs.

References

1. H. Morkoç, R. Cingolania, B. Gil, Polarization effects in nitride semiconductor device structures and performance of modulation doped field effect transistor. Solid-State Electron. **43**, 1753–1771 (1999)
2. Y.C. Lan, X.L. Chen, Y.G. Cao, Y.P. Xu, L.D. Xun, T. Xu, J.K. Liang, Low-temperature synthesis and photoluminescence of AlN. J. Cryst. Growth **207**, 247–250 (1999)
3. I. Vurgaftman, J.R. Meyer, Band parameters for nitrogen-containing semiconductors. J. Appl. Phys. **94**(6), 3675–3696 (2003)
4. R. Aleksan, T. Bolognese, B. Equer, A. Karar, J.M. Reymond, Observation of single minimum ionizing particles with amorphous-silicon diodes. Nucl. Instrum. Methods Phys. Res. Sect. A Accel. Spectrom. Detect. Assoc. Equip. **305**(3), 512–516 (1991)
5. S. Nakamura, Gan growth using Gan buffer layer. Jpn. J. Appl. Phys. Part 2 Lett. **30**(10A), L1705–L1707 (1991)
6. H. Xing, S. Keller, Y.F. Wu, L. McCarthy, I.P. Smorchkova, D. Buttari, R. Coffie, D.S. Green, G. Parish, S. Heikman, L. Shen, N. Zhang, J.J. Xu, B.P. Keller, S.P. DenBaars, U.K. Mishra, Gallium nitride based transistors. J. Phys. Condens. Matter **13**(32), 7139–7157 (2001)
7. V.A.M. Swaminathan, *Materials aspects of Gaas and Inp based structures. Prentice hall advanced reference series* (Prentice Hall, Upper Saddle River, NJ, 1991)
8. N. Van, J.E. Solomon, A. Saxler, Q.H. Xie, D.C. Reynolds, D.C. Look, Dissociation of Al_2O_3(0001) substrates and the roles of silicon and oxygen in n-type GaN thin solid films grown by gas-source molecular beam epitaxy. J. Appl. Phys. **87**(12), 8766–8772 (2000)
9. M. Stutzmann, O. Ambacher, M. Eickhoff, U. Karrer, A.L. Pimenta, R. Neuberger, J. Schalwig, R. Dimitrov, P.J. Schuck, R.D. Grober, Playing with polarity. Phys. Status Solidi B Basic Res. **228**(2), 505–512 (2001)
10. H. Marchand, N. Zhang, L. Zhao, Y. Golan, S.J. Rosner, G. Girolami, P.T. Fini, J.P. Ibbetson, S. Keller, S.D. Baars, J.S. Speck, U.K. Mishra, Structural and optical properties of GaN laterally overgrown on Si(111) by metalorganic chemical vapor deposition using an AlN buffer layer. MRS Internet J. Nitride Semicond. Res. (2014). https://doi.org/10.1557/S1092578300000582
11. M. Seelmann Eggebert, J.L. Weyher, H. Obloh, H. Zimmermann, A. Rar, S. Porowski, Polarity of (00.1) GaN epilayers grown on a (00.1) sapphire. Appl. Phys. Lett. **71**(18), 2635–2637 (1997)
12. S. Nakamura, S. Pearton, G. Fasol, *The blue laser diode* (Springer, Berlin, 2000). https://doi.org/10.1007/978-3-662-0415-7
13. X. Liu, M. Atwater, J. Wang, Q. Huo, Extinction coefficient of gold nanoparticles with different sizes and different capping ligands. Colloids Surf. B **58**(1), 3–7 (2007). https://doi.org/10.1016/j.colsurfb.2006.08.005
14. S. Chichibu, T. Azuhata, T. Sota, S. Nakamura, Spontaneous emission of localized excitons in InGaN single and multiquantum well structures. Appl. Phys. Lett. **69**(27), 4188–4190 (1996). https://doi.org/10.1063/1.116981
15. I. Cekic-Naga, F. Egilmez, G. Ergun, Comparison of light transmittance in different thicknesses of zirconia under various light curing units. J. Adv. Prosthodont. **4**(2), 93–96 (2012). https://doi.org/10.4047/jap.2012.4.2.93
16. Y. Jin, B. Song, Z. Jia, Y. Zhang, C. Lin, X. Wang, S. Dai, Improvement of Swanepoel method for deriving the thickness and the optical properties of chalcogenide thin films. Opt. Express **25**(1), 440–451 (2017)